Visualization and Wake Surveys of Vortical Flow over a Delta Wing

F.M. Payne,* T.T. Ng,† and R.C. Nelson‡
University of Notre Dame, Notre Dame, Indiana
and
L.B. Schiff§
NASA Ames Research Center, Moffett Field, California

An experimental investigation of vortex breakdown on delta wings at high angles of attack is presented. Smoke flow visualization and the laser light sheet technique were used to obtain cross-sectional views of the leading-edge vortices as they break down for a series of flat-plate delta wings having sweep angles of 70, 75, 80, and 85 deg. At low tunnel speeds (as low as 3 m/s), details of the flow that are usually imperceptible or blurred at higher speeds can be clearly seen. A combination of lateral and longitudinal cross-sectional views provides information on the three-dimensional nature of the vortex structure before, during, and after breakdown. Whereas details of the flow are identified in still photographs, the dynamic characteristics of the breakdown process have been recorded using high-speed movies. Velocity measurements have been obtained using a laser Doppler anemometer with the 70 deg delta wing at 30 deg angle of attack. The measurements show that, when breakdown occurs, the core flow is transformed from a jet-like to a wake-like flow.

Introduction

ONE of the most interesting phenomena associated with leading-edge vortices is their breakdown. The breakdown or bursting, as it is commonly called, refers to a sudden and rather dramatic structural change that usually results in the turbulent dissipation of the vortex. Vortex bursting is characterized by a sudden deceleration of the axial flow in the vortex core, the formation of a small recirculatory flow region, a decrease in the circumferential velocity, and an increase in the size of the vortex.

The breakdown of leading-edge vortices has been under study since the late 1950's when research and design work on delta wing aircraft was initiated. Interest in the phenomenon has intensified in recent years as concepts for highly maneuverable aircraft have been developed. These high-performance aircraft are expected to operate routinely at angles of attack at which vortex breakdown is known to occur. When vortex breakdown occurs, the aerodynamic, stability, and control characteristics of the wing change dramatically. Vortex breakdown is a limiting factor on aircraft maneuverability.

Several distinct types of vortex breakdowns have been identified in vortex tube experiments[1]; however, the most common forms of breakdown on wings are the bubble and spiral types. The bubble and spiral modes of vortex breakdown are illustrated in Fig. 1. The bubble or "axisymmetric" mode of vortex breakdown is characterized by a stagnation point on the swirl axis, followed by an oval-shaped recirculation bubble. The bubble is nearly symmetric over most of its length, but the rear is open and asymmetric.

The spiral mode of breakdown is characterized by a rapid deceleration of the core flow followed by an abrupt kink, at which point the core flow takes the form of a spiral that persists for one or two turns before breaking down into large-scale turbulence. For leading-edge vortices, the sense of the spiral has been observed to be opposite to the direction of rotation of the upstream vortex; however, the sense of *rotation* of the spiral is in the same direction as the rotation of the upstream vortex.

In vortex tube experiments in which the vortex swirl speed can be controlled and varied independently of Reynolds number,[1] the spiral type has been found to occur at low values of swirl for a given Reynolds number. As the swirl speed is increased, the spiral form can be seen to transform into the bubble form at a certain critical value of swirl.

Experimental Equipment

All experiments reported in this paper were conducted in the University of Notre Dame's low-turbulence, subsonic smoke wind tunnel. The turbulence intensity is less than 0.1% in the test section throughout the tunnel speed range.

For visualization, smoke was generated by the flash vaporization of deodorized kerosene that was allowed to drip onto electrically heated plates. To illuminate the smoke entrained into the leading-edge vortex system, a laser light source was used. The laser beam was passed through a splitter lens having either a 20 or 60 deg spreading angle. The

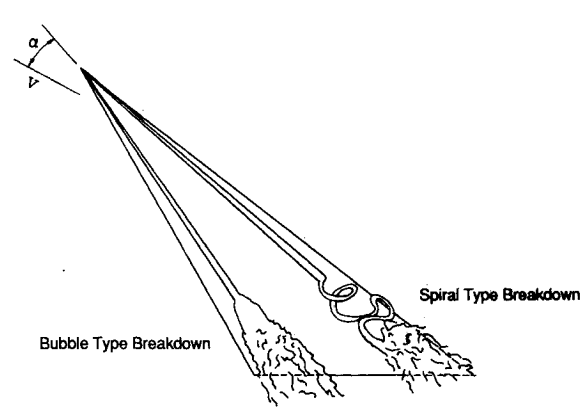

Fig. 1 Flow over a delta wing: bubble and spiral types of vortex breakdown.

Presented as Paper 86-0330 at the 24th AIAA Aerospace Sciences Meeting in Reno, NV, Jan. 6-9, 1986; received June 13, 1986; revision received June 15, 1987.

†Assistant Professor, Aerospace Engineering. Member AIAA.
‡Associate Professor, Aerospace Engineering. Associate Fellow AIAA.
§Research Scientist. Associate Fellow AIAA.

section. The laser light sheet was aligned either normal to the model surface or parallel to the vortices. Additional information on the tunnel and smoke method can be found in Ref. 2.

Four thin sharp-edged delta wings were used in this study. The models each had a root chord of 16 in. (406.4 mm) and were ¼ in. (6.4 mm) thick with sweep angles of 70, 75, 80, and 85 deg. The leading edge was beveled with a 25 deg angle so that a sharp edge was formed on the upper side of the model.

Both still and high-speed motion picture photography was used to record the visual data. A Nikon FM2, 35 mm SLR camera and Kodak Tri-X ASA black-and-white print film were used for the still photographs. For the high-speed movies, a Milliken DBM-5, 16 mm motion picture camera was used. Film frame rates of 500 frames/s (shutter speed 1/1300 s) were used with Eastman 4-X negative film.

Surveys of the vortex flow above the 70 deg swept delta wing were made using a single-component TSI LDA system. A 4 W argon ion laser operating at 514.5 mm was used in conjunction with a beam collimator, 2.27X expander, 50 mm beam splitter, and a 600 mm focusing lens. The nominal beam intersection volume was estimated to be about 2.9 mm in length and 0.14 mm in cross section. The receiving photo detection system had a focal length of 500 mm and the system was positioned at 20–30 deg off-axis in the forward direction. This setup resulted in an estimated measurement probe length of about 1 mm and thickness of about 0.14 mm.

The signal from the receiving optics was amplified and filtered by a TSI 1994 input conditioner and processed by a TSI 1995 counter. The counter was operated on the single measurement/burst mode with 16 cycles/burst. The analog output from the counter was recorded by a PDP 11/23 based data acquisition system with a 12 bit analog/digital converter. By using the Schmitt trigger, 100 samples were collected at each location, except inside the core region where, due to the low particle concentration, 50 samples were taken. With airborne dust particle, the sampling time ranged approximately from 1 min in the outer region to 20 min in the vortex core.

Experimental Results

Flow Visualization Results

Smoke flow visualization and the laser sheet technique were used to study the structure of leading-edge vortices as they broke down. At low freestream velocities (as low as 3 m/s), details of the flow usually imperceptible at higher speeds could be clearly seen. A combination of lateral and longitudinal laser cross-sectional views provided information on the three-dimensional nature of the vortex structure before, during, and after breakdown. Close-up high-speed motion picture photography provided details of the dynamic characteristics of the breakdown process. An attempt was made to classify the observed breakdown modes using these methods.

Early in the investigation it was discovered that operating at relatively low speeds resulted in better resolution of flow features due to a reduced level of turbulence in the test section and a higher density of smoke. For this reason, a freestream velocity of 3 m/s was chosen for all smoke flow visualization tests. This resulted in a Reynolds number based on root chord of approximately 85,000.

One notable consequence of operating at very low speeds (3 m/s) was the tendency of the position of the breakdown to wander on the more highly swept wings. For the lowest sweep wing (70 deg), the breakdown locations of the vortices were approximately symmetric and steady, except for a high-frequency longitudinal oscillation about some mean position. The magnitude of this oscillation was relatively small (less than 2% of the root chord). On the more highly swept wings, the locations of the breakdowns became increasingly

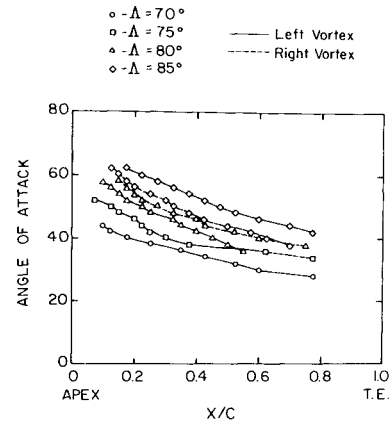

Fig. 2 Location of vortex breakdown ($Re = 425{,}000$).

asymmetric and unsteady in their mean location. On the 85 deg sweep wing, the breakdown location of both vortices was observed to wander forward and aft on the model, apparently at random. However, if the tunnel speed was increased (to say 15 m/s), the unsteadiness in mean position disappeared, although the breakdown positions still tended to be asymmetric. No measurable asymmetry could be identified in the model geometry; however, the accuracy in measurement of yaw angle was approximately ½ deg, which could account for the asymmetric breakdown if the model was misaligned by that amount. In wind-tunnel tests of highly swept delta wings (75–85 deg) at a Reynolds number of 1×10^6, Wentz and Kohlman[3] observed that the breakdown location was quite sensitive to yaw. A misalignment of as little as 0.1 deg was sufficient to cause asymmetric breakdown. In any case, a certain degree of asymmetry is expected with highly swept wings at high angles of attack as the flow past these wings begins to resemble the flow around bodies of revolution at high angles of attack for which symmetric flow has been shown to be unstable. The location of vortex breakdown at 15 m/s for the four wings tested is presented in Fig. 2.

In summary, the wandering of the mean location of breakdown on the 80 and 85 deg wings occurred only at low speeds, but the asymmetry in mean breakdown location for those wings occurred at both low (3 m/s) and relatively high (15 m/s) speeds. The low-magnitude, high-frequency oscillation of the breakdown location occurred for all wings at all speeds tested.

Figure 3a is a photograph of this model at 40 deg angle of attack. A tube of smoke introduced upstream of the contraction cone impinges on the apex of the delta wing and is entrained into the vortices. A 1000 W flood lamp placed outside the test section is illuminating the vortices through the glass side wall of the test section. Both vortices are breaking down about one-third of the way down the model from the apex.

Figure 3b is a multiple-exposure photograph of the 70 deg delta wing using the laser light sheet technique. Vortex cross sections are illuminated by passing the laser beam through a cylindrical lens that splits it into a thin sheet or plane of light. The light sheet then cuts across the test section. In this case, the sheet is perpendicular to the model. The light sheet is expanding at a half-angle of approximately 10 deg. The wing leading edge can be identified by the reflection of the laser sheet on the model surface.

Note the absence of smoke in the core region of the vortices in the two most forward cross sections of Fig. 3b. This lack of smoke can probably be attributed to one or more of the following factors:

1) The smoke is introduced only at the apex of the model; therefore, much of the fluid in the core region is entrained from areas that contain no smoke to begin with.

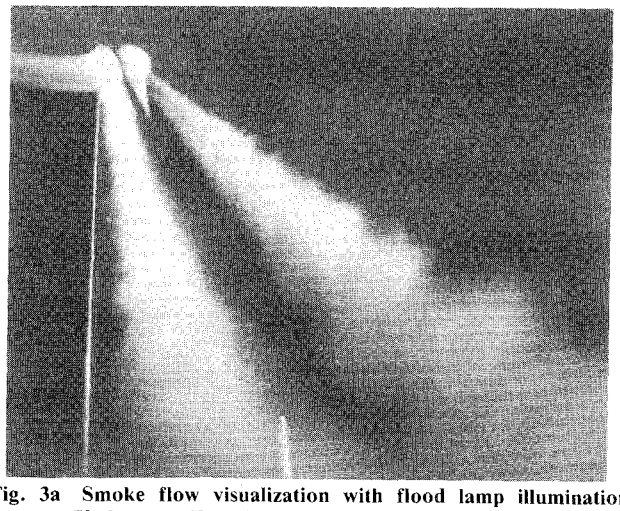

Fig. 3a Smoke flow visualization with flood lamp illumination (sweep = 70 deg, $\alpha = 40$ deg).

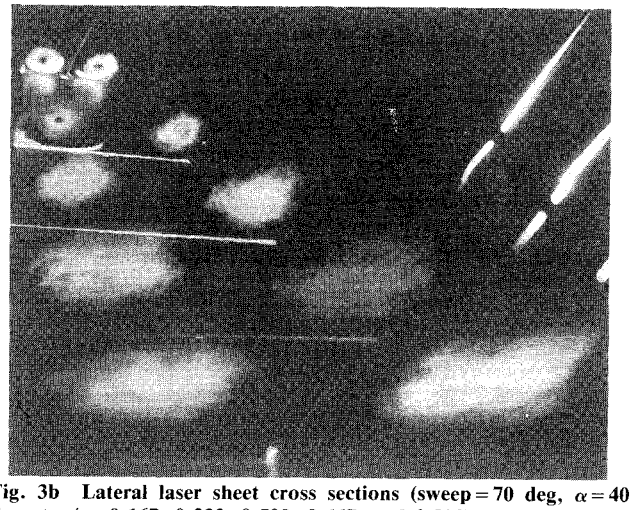

Fig. 3b Lateral laser sheet cross sections (sweep = 70 deg, $\alpha = 40$ deg at $x/c = 0.167$, 0.333, 0.500, 0.667, and 0.833).

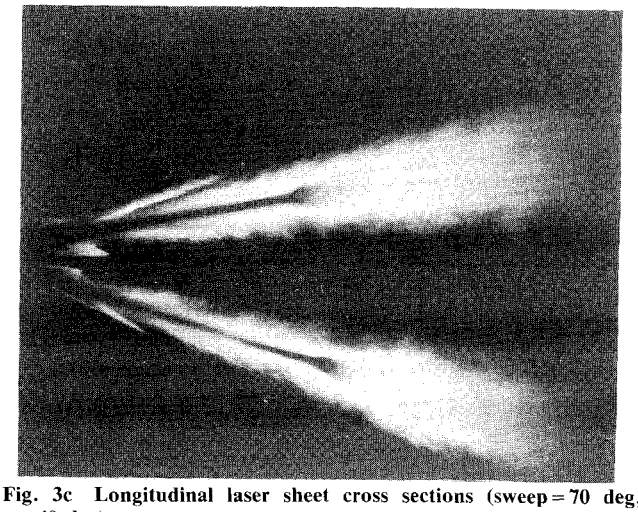

Fig. 3c Longitudinal laser sheet cross sections (sweep = 70 deg, $\alpha = 40$ deg).

2) Velocities in the core can reach approximately three times the freestream value, which reduces the density of smoke entrained into the core.

3) High rotational velocities in the core tend to "spin" smoke particles out.

The first reason may be the most significant because the diameter of the region that is void of smoke was observed to vary depending on where the smoke filament impinged on the model. If the filament impinged on the lower surface below the apex, the void region was seen to increase in diameter. Despite the fact that the void may not correspond to the true diameter of the core, for the sake of simplicity, it will be referred to as the core in the remainder of this paper.

In the forward cross sections of Fig. 3b, the presence of a core indicates that the vortex has not yet broken down. In the third and following cross sections, which are downstream of the breakdown points, no core regions are evident and the vortices appear turbulent and diffuse.

Figure 3c is a photograph of the 70 deg wing at the same conditions as previously stated, except that the laser sheet has been rotated 90 deg to illuminate a longitudinal cross section of the vortices. The dark core region maintains an approximately constant diameter until suddenly expanding just before breaking down. Downstream of the breakdown the vortices are rather featureless.

As progressively higher sweep angles (75, 80, and 85 deg) were tested, it was noted that breakdown occurred farther aft on the models for any given angle of attack. The higher sweep angles also resulted in lower swirl velocities and less diffusion of the smoke, which contributed to clearer and more detailed visualization of the flow features.

In Fig. 4a, the spiral nature of the vortices is visually emphasized by the appearance of striations in the smoke. The striations are believed to be the result of the formation of secondary vortical structures in the vortex shear layer. In the photograph, the vortex on the right is breaking down at approximately the midchord position, while the left vortex does not break down until somewhere in the wake. The combination of high sweep and low freestream velocity usually resulted in asymmetric vortex breakdown, as previously discussed. Which vortex would breakdown first could not be predicted and was observed to change back and forth at irregular intervals. This was probably the result of small changes in the freestream conditions due to gusts or changes in the direction of the wind at the tunnel exit. Without these gusts and changes in wind direction, the turbulence level in the tunnel was less than 0.1%. Lowson[4] observed similar unsteady behavior for very highly swept wings in his water tunnel experiments.

In Fig. 4b, it is possible to actually see the roll-up of the shear layer that forms the primary vortices and the development of the secondary vortical-like structures in the shear layer. The growth of these secondary structures is similar to the evolution of the classic Kelvin-Helmholtz instability. The observed vortical structures are static. They do not rotate with the vortex, but presumably emanate from near the leading edge and follow a spiral path that is fixed with respect to the shear layer.

It is interesting to note that, when the smoke stream drifted away from the apex of the wing, it was sometimes entrained into the region between the feeding sheet and the core. When this occurred, the shear layer vortices appeared as dark areas void of smoke, but was still identifiable by their outlines. The fact that this occurred supports the conclusion that the observed structures are associated with the flow and not merely a consequence of the visualization method.

In Fig. 4c, it is the right vortex that is breaking down. Details in the recirculation zone or "bubble" region are clearly visible. Note that the vortices curve slightly away from the wing ("out" of the photograph) and, since the laser sheet is planer, the laser cross section cuts at an angle through the vortices. This is why the core region is visible for only a portion of the entire cross section. The direction of the spiral on the right side of the lower vortex indicates the laser sheet is cutting across the underside of the vortex at that point.

An extremely useful tool in the analysis of complicated flows is the motion picture camera. In order to obtain a better understanding of the breakdown structure, a Milliken

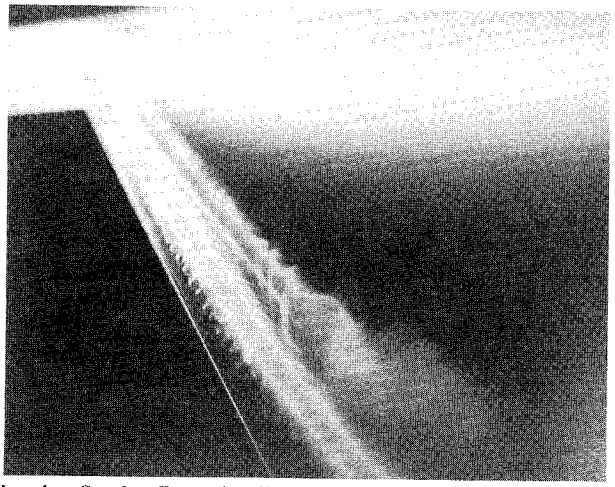

Fig. 4a Smoke flow visualization with flood lamp illumination (sweep = 85 deg, $\alpha = 40$ deg).

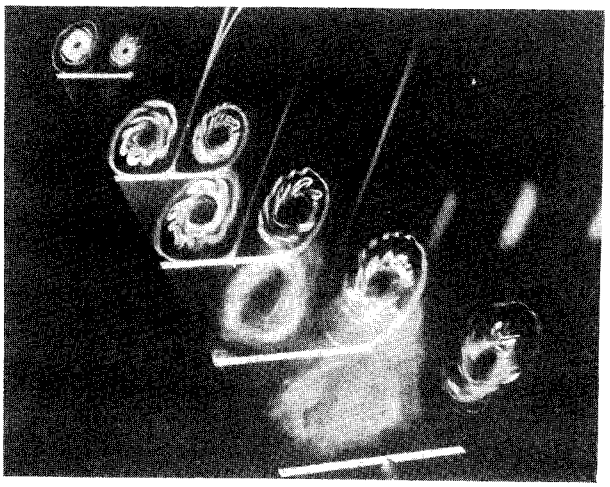

Fig. 4b Lateral laser sheet cross sections (sweep = 85 deg, $\alpha = 40$ deg at $x/c = 0.167$, 0.333, 0.500, 0.667, and 0.833).

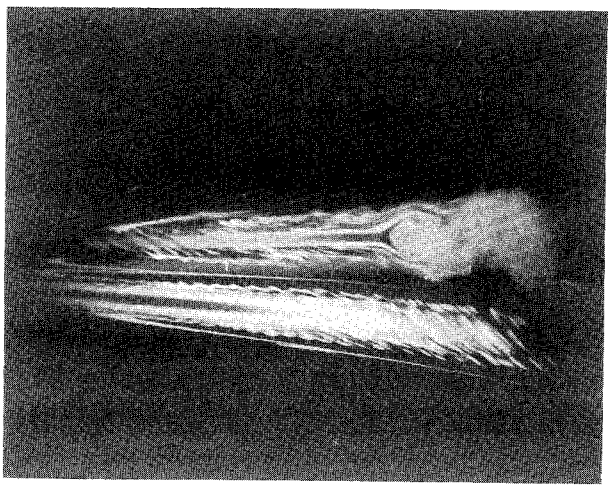

Fig. 4c Longitudinal laser sheet cross section (sweep = 85 deg, $\alpha = 40$ deg).

high-speed movie camera was used to photograph the phenomenon at 500 frames/s. The effective shutter speed for a single frame was 1/1300 s. In Figs. 5–8, single frames from the 16 mm movies have been isolated and enlarged. The photographs are longitudinal and lateral laser sheet cross sections of vortex breakdown on the 85 deg delta wing. Accompanying the photographs are sketches depicting the salient features observed in the movie frames.

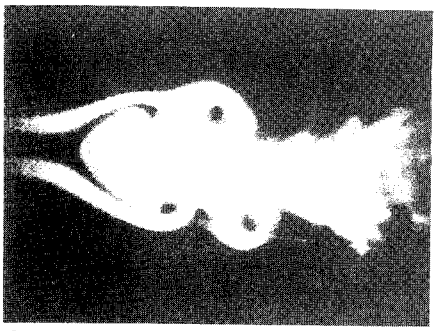

Fig. 5a Enlargement from 16 mm movie frame of a bubble-type breakdown (longitudinal cross section, sweep = 85 deg, $\alpha = 40$ deg).

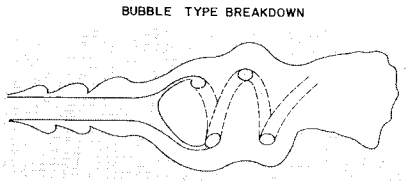

Fig. 5b Schematic representation of a bubble-type breakdown (longitudinal cross section).

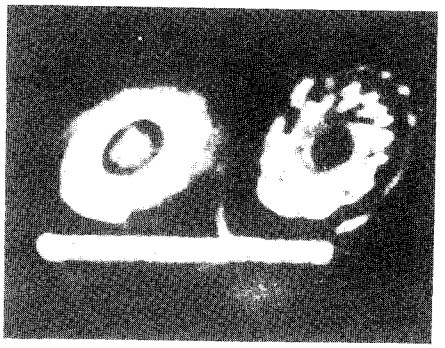

Fig. 6a Enlargement from 16 mm movie frame of a bubble-type breakdown (lateral cross section, sweep = 85 deg, $\alpha = 40$ deg).

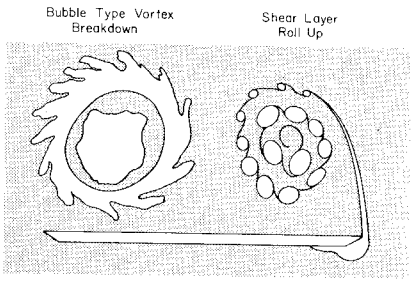

Fig. 6b Schematic representation of a bubble-type breakdown (lateral cross section).

One of the goals of this study is to identify the type or types of breakdown that occur on sharp-edged delta wings at these Reynolds numbers; however, a certain amount of caution must be exercised when interpreting flow visualization results. What is not seen may be just as important as what is seen. The still photographs described above, together with the high-speed motion pictures, can be interpreted in various ways. The particular ambiguity that makes a definite identification of the breakdown process difficult in this case is that the smoke in these photographs is entrained into the outer region of the vortex and not into the core—and it is the behavior of the core that is of primary interest. The core behavior must be inferred by observing a region void of smoke. With this difficulty in mind, two possible breakdown forms will be described.

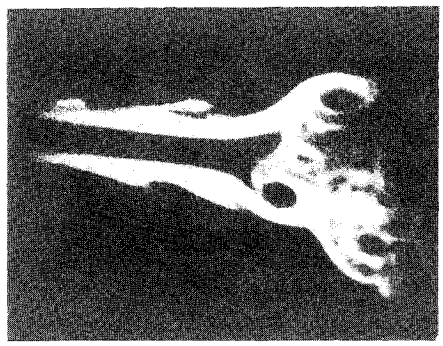

Fig. 7a Enlargement from 16 mm movie frame of a spiral-type breakdown (longitudinal cross section, sweep = 85 deg, $\alpha = 40$ deg).

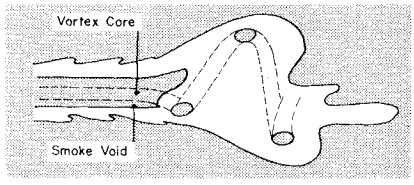

Fig. 7b Schematic representation of a spiral-type breakdown (longitudinal cross section).

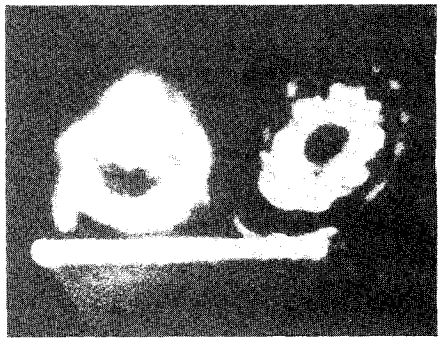

Fig. 8a Enlargement from 16 mm movie frame of a spiral-type breakdown (lateral cross section, sweep = 85 deg, $\alpha = 40$ deg).

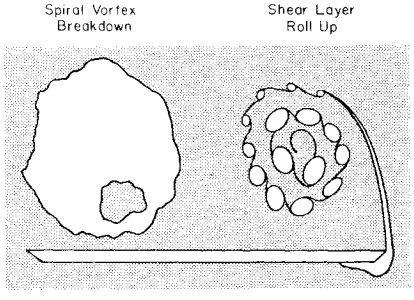

Fig. 8b Schematic representation of a spiral-type breakdown (lateral cross section).

The first type of breakdown process resembles the bubble form described in vortex tube experiments found in the literature. In Fig. 5, the core flow seems to expand around an oval-shaped recirculation zone. At the exit of this recirculation zone, the core flow appears to shed in the form of vortex rings that are then convected downstream. The "vortex rings" are, in fact, a consequence of a tightly wound spiral tail that emanates from the aft end of the bubble. Figure 6 is a lateral cross section of the bubble-type breakdown. The bubble was sometimes nearly symmetric, but often highly asymmetric and almost constantly changing.

The breakdown process occurring above was occasionally observed to change into what might be interpreted as a spiral mode. When this occurred, the mean location of the breakdown moved downstream and took the form depicted

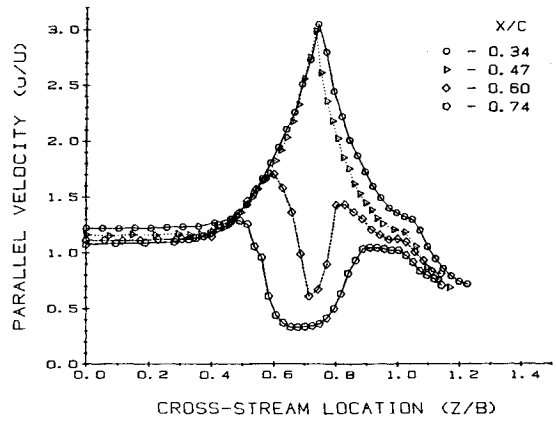

Fig. 9 Parallel velocity component profiles for various axial locations (sweep = 70 deg, $\alpha = 30$ deg).

in Fig. 7. The large recirculation zone has disappeared and the core flow now appears to corkscrew downstream. In this case, the holes in the flow are assumed to be cross sections of the spiraling core flow. This type of result was also obtained in wind-tunnel tests at ONERA using the laser sheet technique.[5] In that study, "holes" appearing in the wake of a breakdown were also observed and interpreted to be cross sections of the spiraling vortex core. Figure 8 shows a lateral cross-section which appears to show a rotating core. After a short time, this spiral mode would transform back into the "bubble" form and move upstream. The transformation from bubble to spiral was not instantaneous, but involved a continuous sequence of intermediate forms that are difficult to classify as either bubble or spiral.

This behavior is in agreement with that observed by Lowson[4] in water-tunnel experiments with an 80 deg sweep delta wing. Lowson observed that, for a highly swept delta wing, the breakdown position was both asymmetric and unsteady (at $Re = 30{,}000$) and that the breakdown took the form of a bubble when moving forward (upstream) and a spiral when moving aft.

LDA Results

Most measurements to date on vortex breakdown were obtained from experiments inside ducts or on delta wings. Due to the susceptibility of the breakdown to probe interference, nonintrusive measurement techniques such as laser Doppler anemometer (LDA) are preferred over physical measurement probes. For example, Faler and Leibovich[1] and Escudier and Zehnder[6] measured the velocity field of the axisymmetric vortex breakdown of a swirling flow inside a circular duct using LDA. The interior of the recirculation zone was found to be dominated by low-frequency, nonaxisymmetric fluctuations. Measurements of the flow above a delta wing were performed by Anders[7] and Verhaagen and Kruisbrink[8] using LDA. In general, all of the experimental data indicate that, in an axisymmetric breakdown, the core flow evolves from jet-like to wake-like behavior, with the presence of a recirculation "bubble" signifying the transition.

LDA measurements of the velocity components parallel and normal to the wing surface were made for the 70 deg swept delta wing at a 30 deg angle of attack for a freestream velocity of 10 m/s. The spanwise surveys were taken in the plane of the vortex core centers. Figures 9–12 summarize the velocity components and root mean square (rms) velocity profiles..

Since the LDA data were taken without frequency shifting, one of the major sources of error was the inability of the system to resolve low velocity and reversal velocity. This would result in a higher-than-actual mean velocity and lower-than-actual rms velocity under certain flow situations. Another source of error was due to the finite-measurement probe size. Within these limitations, the measurements were

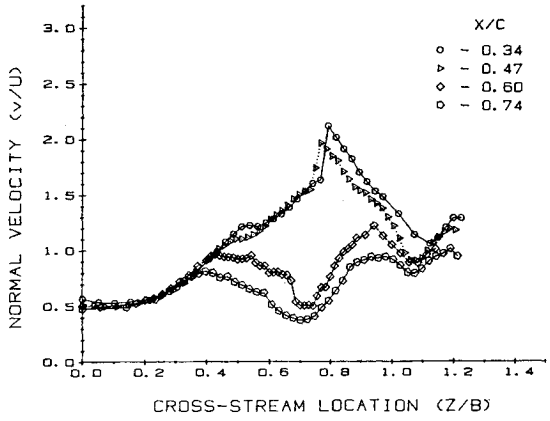

Fig. 10 Normal velocity component profiles for various axial locations (sweep = 70 deg, $\alpha = 30$ deg).

repeated several times to ensure repeatability. The variation encountered among the profiles was in the order of 5%.

Figure 9 shows that the core velocity initially accelerated until the maximum axial velocity upstream of the breakdown reached a value about three times the freestream velocity. The velocity peak was relatively narrow and pointed when compared with similar measurements inside ducts such as in Faler and Leibovich.[1] Breakdown of the vortex occurred between stations $x/c = 0.47$ and 0.54, during which the axial velocity profile evolved from a jet-like into a wake-like flow. This behavior corresponds with what has been commonly observed for "bubble" type of breakdown. Under this flow condition, the "bubble" mode is the dominant one; however, measurements at several more closely spaced locations around the breakdown are needed before more details of the process can be revealed. Furthermore, the unsteadiness in the breakdown location may warrant some form of conditional sampling technique to be used. As opposed to flow inside ducts, the vortex over the delta wing was not symmetric about its axis. This nonsymmetric behavior was shown more clearly by the velocity component normal to the wing surface depicted in Fig. 10. The magnitude of the normal velocity was higher at the part of the vortex nearer the edge of the wing. Part of the nonsymmetry was due to the fact that the LDV probe was traversed parallel to the trailing edge instead of normal to the vortex axis; however, since the streamwise evolution is relatively slow (except near breakdown), the conclusion of asymmetry based on the present data would still be valid. While this asymmetry may not alter significantly the physical mechanisms governing the breakdown process, the parametric dependence would be affected. It also made studying the flow more difficult, both analytically and experimentally. After breakdown, the normal velocity diminished in magnitude as the cross section of the vortex increased. These mean velocity distributions agree very well with those of Anders.[7]

The rms velocity fluctuations are shown in Figs. 11 and 12. Before breakdown, the velocity fluctuations near the core of the vortex tube showed a narrow peak with a maximum value of about 30% of the freestream velocity. Outside of the center region, the rms velocity was relatively uniform, with another peak outboard of the wing where the shear layer rolled up from the leading edge. The rms peak became narrower relative to the vortex tube cross section as the flow proceeded to breakdown. After breakdown, the rms velocity acquired a strong, double-peaked distribution in the parallel component. Farther downstream from the breakdown point, the flow transitioned to turbulent flow and the mean and rms velocities assumed distributions more typical of a wake flow. Later measurements with frequency shifting revealed that the swirl velocity switched direction over a very short span across the core, resulting in a very steep normal velocity gradient near the center of the core before breakdown.

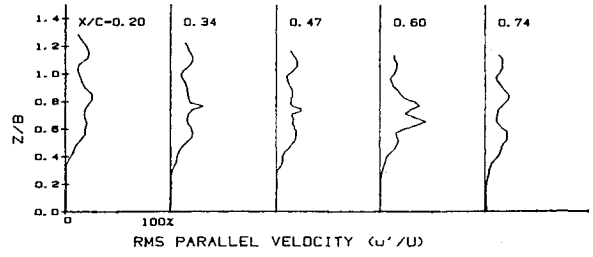

Fig. 11 Root mean square parallel velocity component profiles for various axial locations (sweep = 70 deg, $\alpha = 30$ deg).

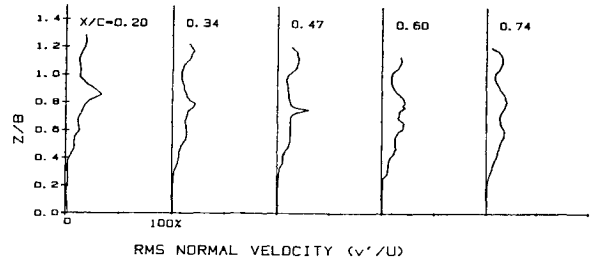

Fig. 12 Root mean square normal velocity component profiles for various axial locations (sweep = 70 deg, $\alpha = 30$ deg).

Therefore, the observed high rms velocity peak near the core could be a result of the wandering of the vortex about a fixed measurement position or it could be the actual fluctuations of the velocity field in the vortex, or a combination of both. This issue, however, cannot be resolved with the present data, although the flow visualization photographs did indicate a rather stable internal vortex structure before breakdown.

Conclusion

Smoke flow visualization and the laser sheet technique have been shown to be effective tools in the study of vortical flowfields. The position of leading-edge vortices and the location of their breakdown at high angles of attack can be determined. Details of the breakdown process have been studied using still and high-speed motion picture photography.

The following observations were made conserning vortex breakdown on delta wings at low Reynolds number:

1) At a given angle of attack, as the sweep angle is increased, the location of breakdown moves aft.

2) For a given set of conditions, the breakdown location oscillated at high frequency about a mean position and for highly swept wings (sweep = 80–85 deg) at low speeds, the mean position will migrate considerably forward and aft on the models.

3) High-speed films revealed what appears to be two types of breakdown on the 85 deg wing, a bubble mode and a spiral mode. The two modes were seen to transform from one to the other apparently at random, with the bubble form seeming to prefer a more upstream location relative to the spiral mode. The existence of more than one mode of breakdown, as well as their behavior with respect to preferred location, is consistent with observations of vortex breakdown in tubes reported in the literature.

4) Velocity profiles obtained with a laser anemometer showed the development of a jet-like core flow that reached three times the freestream velocity before breaking down. After the breakdown, the velocity profiles became wake-like in nature.

Acknowledgment

This research is being supported by NASA Ames Research Center under NASA Grant NAG-2-258 and the University of Notre Dame.

References

[1]Faler, J.H. and Liebovich, S., "Disrupted States of Vortex Flow and Vortex Breakdown," *The Physics of Fluids,* Vol. 20, 1977, pp. 1385–1400.

[2]Payne, F.M., Ng, T.T., Nelson, R.C., and Schiff, L.G., "Visualization and Flow Surveys of the Leading Edge Vortex Structure on Delta Wing Planforms," AIAA Paper 86-0330, Jan. 1986.

[3]Wentz, W.H. and Kohlman, D.L., "Vortex Breakdown on Slender Sharp-Edged Wings," *Journal of Aircraft,* Vol. 8, March 1971.

[4]Lowson, M.V., "Some Experiments with Vortex Breakdown," *Journal of the Royal Aeronautical Society,* Vol. 68, May 1964.

[5]Werle, H., "Flow Visualization Techniques for the Study of High Incidence Aerodynamics," AGARD LSP-121, March 1982, pp. 3-1—3-24.

[6]Escudier, M.P. and Zehnder, N., "Vortex-flow Regimes," *Journal of Fluid Mechanics,* Vol. 115, 1982, pp. 105–121.

[7]Anders, K., "LDV Measurements of the Velocity Field of a Leading Edge Vortex over a Delta Wing before and after Vortex Breakdown," Von Kármán Institute for Fluid Mechanics, Brussels, Tech. Note 142-7, March 1982.

[8]Verhaagen, N.G. and Kruisbrink, A.C.H., "The Entrainment Effect of a Leading Edge Vortex," AIAA Paper 85-1584, July 1985.